


RESEARCH ARTICLE

People with obesity exhibit losses in muscle proteostasis that are partly improved by exercise training

Kanchana Srisawat¹ | Connor A. Stead¹ | Katie Hesketh¹ | Mark Pogson¹ | Juliette A. Strauss¹ | Matt Cocks¹ | Ivo Siekmann² | Stuart M. Phillips³ | Paulo J. Lisboa² | Sam Shepherd¹ | Jatin G. Burniston¹ 

¹Research Institute for Sport, & Exercise Sciences, Liverpool, UK

²Department of Applied Mathematics, Liverpool John Moores University, Liverpool, UK

³Department of Kinesiology, McMaster University, Hamilton, Ontario, Canada

Correspondence

Jatin G. Burniston, Research Institute for Sport, & Exercise Sciences (RISES), Liverpool Centre for Cardiovascular Science (LCCS) Liverpool John Moores University, Tom Reilly Building, Liverpool, L3 3AF, UK.
Email: j.burniston@ljmu.ac.uk

Present address: Kanchana Srisawat, Department of Disease Control, Ministry of Public Health, Nonthaburi, Thailand. Katie Hesketh, School of Sport, Exercise and Rehabilitation Sciences, University of Birmingham, Birmingham, B15 2FG, UK, and Mark Pogson, Department of Communication and Media, University of Liverpool, Liverpool, L69 3BX

Funding information

Royal Thai Government

Abstract

This pilot experiment examines if a loss in muscle proteostasis occurs in people with obesity and whether endurance exercise positively influences either the abundance profile or turnover rate of proteins in this population. Men with ($n = 3$) or without ($n = 4$) obesity were recruited and underwent a 14-d measurement protocol of daily deuterium oxide (D_2O) consumption and serial biopsies of vastus lateralis muscle. Men with obesity then completed 10-weeks of high-intensity interval training (HIIT), encompassing 3 sessions per week of cycle ergometer exercise with 1 min intervals at 100% maximum aerobic power interspersed by 1 min recovery periods. The number of intervals per session progressed from 4 to 8, and during weeks 8–10 the 14-d measurement protocol was repeated. Proteomic analysis detected 352 differences ($p < 0.05$, false discovery rate $< 5\%$) in protein abundance and 19 ($p < 0.05$) differences in protein turnover, including components of the ubiquitin-proteasome system. HIIT altered the abundance of 53 proteins and increased the turnover rate of 22 proteins ($p < 0.05$) and tended to benefit proteostasis by increasing muscle protein turnover rates. Obesity and insulin resistance are associated with compromised muscle proteostasis, which may be partially restored by endurance exercise.

KEYWORDS

biosynthetic labelling, deuterium oxide, fractional synthesis rate, heat shock proteins, heavy water, muscle protein synthesis, protein turnover, proteomics, skeletal muscle, ubiquitin proteasome system

Abbreviations: ADH1, alcohol dehydrogenase 1; ATP, adenosine triphosphate; BMI, body mass index; C(I-V), complex (I-V) of the mitochondrial respiratory chain; D_2O , deuterium oxide (2H_2O); DEXA, dual-energy x-ray absorptiometry; FA, formic acid; FAO, fatty acid oxidation; FSR, fractional synthesis rate; HIIT, high-intensity interval training; HSP, heat shock protein; sHSP, small heat shock protein; KEGG, Kyoto encyclopedia of genes and genomes; m_0 , monoisotopic peak; mTORC1, mammalian/mechanistic target of rapamycin, complex 1; NHS, National Health service; NWC, normal-weight control; OGTT, oral glucose tolerance test; OIR, obese insulin resistant; OXPHOS, oxidative phosphorylation; PRDX, peroxiredoxin; NADH, nicotinamide adenine dinucleotide; SDH, succinate dehydrogenase; STRING, search tool for the retrieval of interacting genes/proteins; TCA, tricarboxylic acid; UPLC, ultra-performance liquid chromatography; VO_2 , oxygen uptake; W_{max} , maximum aerobic power (W).

Kanchana Srisawat and Connor A. Stead contributed equally to this work.

This is an open access article under the terms of the [Creative Commons Attribution](https://creativecommons.org/licenses/by/4.0/) License, which permits use, distribution and reproduction in any medium, provided the original work is properly cited.

© 2023 The Authors. *Proteomics* published by Wiley-VCH GmbH.

1 | INTRODUCTION

The pathogenesis of obesity and type II diabetes is underpinned by defects in metabolic homeostasis, including hyperinsulinemia and insulin resistance [1]. However, there is uncertainty regarding the effects of obesity and insulin resistance on protein metabolism in human muscle [2]. Gains in muscle mass can coincide with the elevation in fat mass associated with obesity, but people with obesity are also more susceptible to age-related muscle loss (i.e., sarcopenic obesity). Chronically elevated insulin signalling dampens muscle glucose uptake but other aspects of the insulin receptor signalling cascade, including mTORC1 activation and subsequent effects on protein turnover, may remain stimulated [1]. Indeed, kinase activity profiling [3] found evidence of hypo-activation of negative regulators of the mTORC1 pathway in the muscle of people with obesity and insulin resistance.

Protein turnover is essential to protein homeostasis (proteostasis) but under fasting conditions [4, 5] or in the post-absorptive state [6], the turnover of mixed protein may be lower in the muscle of people with obesity. When proteins of the myofibrillar fraction are studied, no differences in protein turnover are evident between individuals with or without obesity, but healthy-weight individuals have a greater rise in myofibrillar protein fractional synthesis rate (FSR) after a protein-rich meal [7]. The average FSR of proteins in the muscle mitochondrial fraction is also less in people with obesity [6, 5], but the protein synthetic response to amino acids may be either impaired [6] or enhanced [5]. In part, the lack of consensus regarding the effects of obesity on muscle protein turnover could arise due to the lack of protein specific detail.

The abundance profile of proteins is different between the muscle of people with and without obesity [8], and proteins with different functions have different turnover rates in human muscle [9]. Moreover, the connection between gene expression and protein abundance is dysregulated in obesity, which implies differences in either protein translation or degradation. In the muscle of people with obesity, mitochondrial proteins are downregulated at both the transcript and protein level, whereas, the down regulation of transcripts relating to protein translation and amino acid metabolism is not evident at the protein level [10]. There are also blunted and disparate transcriptome, proteome, and phosphoproteome responses to acute aerobic exercise in the muscle of people with obesity [10], which may impact their responsiveness to exercise training.

The above observations implicate dysregulation of muscle protein turnover in the context of obesity and question whether protein-specific responses may occur rather than changes *en masse* to the turnover of muscle proteins. While it is challenging to measure the turnover of individual proteins using isotope-labelled amino acid tracers in humans, the stable isotope deuterium oxide (D_2O) can be readily combined with peptide mass spectrometry to generate robust data on the synthesis rate and abundance of each protein [11]. The current study used D_2O labelling and proteomics to investigate differences in the turnover and abundance of muscle proteins between men with and without obesity. We hypothesized that obesity is associated with select differences in the turnover, as well as abundance, of proteins in

Significance Statement

Skeletal muscle dysfunction contributes to the metabolic abnormalities in people with obesity, but it is uncertain whether the turnover of muscle proteins is increased or decreased. This study demonstrated that humans with obesity exhibit widespread alterations in the abundance and turnover rate of individual muscle proteins. Fundamental components of the proteostasis network, including the ubiquitin proteasome system and heat-shock protein chaperones, featured prominently amongst the differences between the muscle proteomes of people with and without obesity. Ten weeks of high-intensity interval exercise training tended to improve muscle proteostasis in people with obesity but did not fully mitigate indicators of poor proteome health.

human muscle, and that a programme of aerobic exercise would restore muscle proteostasis.

2 | MATERIALS AND METHODS

2.1 | Study design

Normal-weight men ($n = 4$) and men with obesity ($n = 3$) between the ages of 30–45 years were recruited. Each participant gave their informed consent to the experimental procedures approved (16/WM/0296) by the Black Country NHS Research Ethics Committee (West Midlands, UK) and conformed with the Declaration of Helsinki, except registration in a clinical trials database. Anthropological and physiological data were collected at least 3 days prior to commencing the first 14-day period of D_2O consumption (i.e., baseline investigation period). Throughout baseline measurements, saliva and blood samples were collected, and muscle samples were obtained before D_2O administration (0 day) and after 4, 9, and 14 days of D_2O consumption. Normal-weight participants completed the baseline investigation only, whereas the men with obesity also undertook a 10-week HIIT intervention. During the final 2 weeks of the HIIT intervention (weeks 8 to 10), participants consumed D_2O and samples were collected consistent with the baseline investigation (Figure 1). Physiological measurements were repeated in men with obesity at least 72 h after completing the 10-week HIIT intervention.

2.2 | Physiological assessment

Body composition was measured using dual-energy x-ray absorptiometry (DEXA; Hologic QDR Series). Maximal aerobic power (W_{max}) and peak oxygen uptake (VO_{2peak}) were determined using a progressive exercise test to exhaustion [12] on an electronically braked cycle

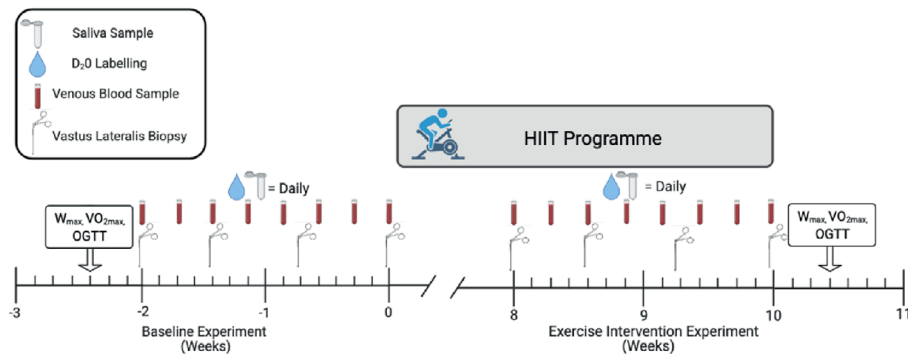


FIGURE 1 Experimental design. A 2-week deuterium oxide (D₂O) labelling experiment was conducted with normal-weight healthy control (NWC; $n = 4$) and obese insulin resistant (OIR; $n = 3$) participants to collect baseline data (weeks -2 – 0). Saliva sampling and D₂O administration (4×50 mL) were conducted daily and venous blood samples were collected every other day. Percutaneous biopsies of vastus lateralis muscle were conducted on days 0, 4, 9, and 14. The OIR group then completed a 10-week high-intensity interval training (HIIT) program. During the last 2 weeks of the training intervention, a repeat of the labelling experiment was conducted to investigate the effects of exercise on the OIR muscle proteome. Physiological data, including peak aerobic power (W_{\max}), peak oxygen uptake ($VO_{2\text{peak}}$) and oral-glucose tolerance (OGTT), were measured 72 h prior to the collection of baseline biological samples or 72 h after completion of the 10-week HIIT intervention.

ergometer (Lode BV). The initial load was 95 W for 3 min, followed by increments of 35 W every 3 min until cadence was reduced to < 50 rpm. Respiratory gasses were measured using a metabolic cart (Moxus), $VO_{2\text{peak}}$ was recorded as the highest value during the last 30 s of the test. On a separate occasion, insulin sensitivity was assessed by oral glucose tolerance test (OGTT) after an overnight fast (> 10 h), and after having refrained from vigorous exercise in the preceding 48 h period.

2.3 | HIIT protocol

After a 3-min warm-up cycling at 50 W, participants performed repeated cycling bouts at 100% maximum power output (W_{\max}) for 60 s, interspersed with 60 s low-intensity recovery cycling at 50 W, maintaining a cadence < 50 rpm. Participants trained three times per week for 10 weeks. Initially, participants performed four intervals per session, which increased by one interval after every 2 weeks of training, such that participants performed 8 intervals per session during weeks 9 and 10.

2.4 | Stable isotope labelling in vivo

Participants consumed 50 mL of 99.8 atom % of deuterium oxide (D₂O; Sigma-Aldrich) four times per day (200 mL per day) approximately 3–4 h apart, during each 14-day labelling period. Body water D₂O enrichment was measured in plasma and saliva samples using gas chromatography-mass spectrometry after exchange with acetone, as described previously [9].

2.5 | Muscle analysis

Muscle biopsies were performed after an overnight fast (> 10 h) on day 0, 4, 9, and 14 of each labelling period. Local anaesthetic (0.5%

Marcaïne) was administered and samples (~ 100 mg) of vastus lateralis muscle were obtained by conchotome, snap-frozen in liquid nitrogen and stored at -80°C for subsequent analysis. Participants received two muscle biopsies from each leg in a randomized order over the 14-day experimental periods.

Muscles were processed to myofibrillar and soluble fractions according to routine methods optimized for skeletal muscle [9]. Protein concentrations were measured by Bradford assay and tryptic digestion was performed overnight. Samples containing 4 μg of peptides were de-salted using C₁₈ Zip-tips (Millipore) and resuspended in 20 μL of 2.5% (v/v) ACN, 0.1% (v/v) FA containing 10 fmol/ μL yeast alcohol dehydrogenase (ADH1; Waters Corp.).

Myofibrillar fractions were analysed using a NanoAcquity UPLC system (Waters Corp.) and Q-TOF Premier mass spectrometer (Waters Corp.), whereas soluble muscle proteins were analysed using an Ultimate 3000 nano system (Thermo Scientific) coupled to a Fusion mass spectrometer (Thermo Scientific). In each case, samples were separated by RP chromatography over a duration of 90 min and the mass spectrometer settings were optimized for label-free quantitation of peptide mass spectra. Further details are provided in the online Supporting Information.

Mass spectrometry raw files were processed using Progenesis Quantitative Informatics for proteomics version 4.2 (Waters Corp.) consistent with our previous work [9]. MS/MS spectra in Mascot generic format were searched against the Swiss-Prot database restricted to Homo-sapiens (20,272 sequences) using a locally implemented Mascot server (v.2.8; www.matrixscience.com). Enzyme specificity was trypsin (1 missed cleavage), carbamidomethyl modification of cysteine (fixed) and oxidation of methionine (variable). QTOF data were searched using m/z errors of 0.3 Da, FUSION data were searched using MS error 10 ppm and MS/MS error 0.6 Da. Protein abundances were calculated using nonconflicting peptides and normalized to the three most abundant peptides of yeast ADH1 to derive abundance measurements in fmol/ μg protein.

2.6 | Measurement of protein synthesis rates

Protein fractional synthesis rates (FSR) were calculated per our previous work [9]. The incorporation of deuterium into newly synthesized protein causes a decrease in the molar fraction of the peptide monoisotopic (m_0) peak [13]. Changes in mass isotopomer distribution follow a nonlinear bi-exponential pattern due to the rise-to-plateau kinetics in D_2O enrichment of the body water compartment (measured in plasma samples by GC-MS) and the rise-to-plateau kinetics of D_2O -labelled amino acids into newly synthesized protein (measured in muscle proteins by LC-MS). Data were fitted using a machine learning approach to optimize for the rate of change in the relative abundance of the monoisotopic (m_0) peak. The rate of change in mass isotopomer distribution is also a function of the number of exchangeable H sites; this fact was accounted for by referencing each peptide sequence against standard tables that reported the relative enrichment of amino acids by deuterium in humans.

2.7 | Statistical and bioinformatic analysis

Statistical analysis was performed in R (Version 3.6.2). Baseline protein abundances were calculated in each participant from the median abundance of each protein across the time-series, whereas post-exercise protein abundances were quantified from the final biopsy only.

Baseline comparisons of participant physiological data, protein abundances, and protein turnover rates between the NWC and OIR groups were analysed using between-subjects ANOVA. Whereas within-subjects ANOVA was used to assess differences between baseline and post-exercise measures in OIR participants. Significance was identified as $p < 0.05$. False-discovery rates (q-values) were calculated for all protein data to test for false positives. Gene ontology analysis (GO) and protein interactions were investigated using the search tool for the retrieval of interacting genes/proteins (STRING) [14].

3 | RESULTS

3.1 | Participant health and exercise characteristics

Due to the nature of the protocols used in this pilot investigation a sample size of $n = 4$ normal-weight and $n = 3$ males with obesity completed all protocols and were analysed. Participants were Caucasian from the Liverpool City region, and their physiological data are reported in Table 1. Normal-weight participants and those with obesity had a BMI of $24.2 \pm 2.4 \text{ kg/m}^2$ and $34.0 \pm 5.8 \text{ kg/m}^2$, respectfully. Participants with obesity had a significantly ($p < 0.01$) lower $VO_{2\text{peak}}$ and W_{max} compared to normal-weight individuals (Table 1). Fasting insulin concentrations tended ($p = 0.07$) to be greater in people with obesity, but fasting blood glucose levels were

not different between the groups. In response to the OGTT, the area under the curve (AUC) of plasma glucose was similar between groups, whereas for the AUC of insulin tended to be greater in people with obesity. Participants with obesity were classified as insulin-resistant based on Matsuda Index (MI; $1.7 \pm 0.6 \text{ mmol}$), which was significantly ($p < 0.01$) less than normal-weight participants ($5.7 \pm 1.4 \text{ mmol}$). Based on the above characteristics, the abbreviations obese insulin resistant (OIR) and normal-weight controls (NWC) are used throughout the manuscript when referring to the groups of people with and without obesity.

After 10-weeks of HIIT, the $VO_{2\text{peak}}$ of OIR participants increased by 9% and W_{max} increased 14 % (Table 1). There was no change in fat mass or body fat percentage and HIIT did not significantly alter fasting concentrations of glucose or insulin. The mean glucose and insulin AUC were less in response to OGTT after the 10-week exercise programme, but these improvements did not reach statistical significance. Similarly, the Matsuda index of OIR participants (2.0 ± 1.0) was 18% greater than baseline (1.7 ± 0.6) after the HIIT intervention, this improvement in insulin sensitivity also did not reach statistical significance.

3.2 | Dynamic proteome profiling of human muscle

Deuterium enrichment of body water rose at a rate of $0.25 \pm 0.06\%/d$ to a maximum of $3.54 \pm 0.5\%$ during the first 14-day measurement period. After 8 weeks without deuterium oxide consumption (i.e., day 0 of the second measurement period), body-water enrichment of deuterium had returned to 0.08%. During the second 14-day measurement period, deuterium enrichment of body-water rose at a rate of $0.22 \pm 0.07\%/d$ to a maximum of $3.11 \pm 0.5\%$. There were no significant differences in the rate of body-water enrichment calculated from measurements made using equivalent plasma or saliva samples (data not shown). Proteomic analysis encompassed 40 muscle samples, including day 0, 4, 9, and 14 time points at baseline ($n = 4$ NWC and $n = 3$ OIR) and day 0, 4, 9, and 14 time points during weeks 8 to 10 of the HIIT intervention ($n = 3$, OIR only). Overall, 1422 proteins were confidently identified and after filtering to exclude missing values amongst biological replicates, the abundance of 919 proteins was measured across all sampling times in at least $n = 3$ participants per group. Protein abundances were stable (Figure 2A) in each participant across each time-series (day 0, 4, 9, and 14) of samples used to investigate the biosynthetic labelling of proteins with deuterium. OIR and NWC participants were separated by principal component analyses of protein abundance data (Figure 2C) and between group ANOVA highlighted 352 significant ($p < 0.05$, $q < 0.05$) differences in protein abundance, including 289 proteins that were more abundant in OIR and 63 that were more abundant in NWC muscle at baseline (Figure 2G, Table S1). In addition, within-subject ANOVA of day 0 baseline samples and samples taken after 10 weeks HIIT in OIR participants highlighted 53 statistically significant ($p < 0.05$) changes in protein abundance, including 33 proteins that increased and 20

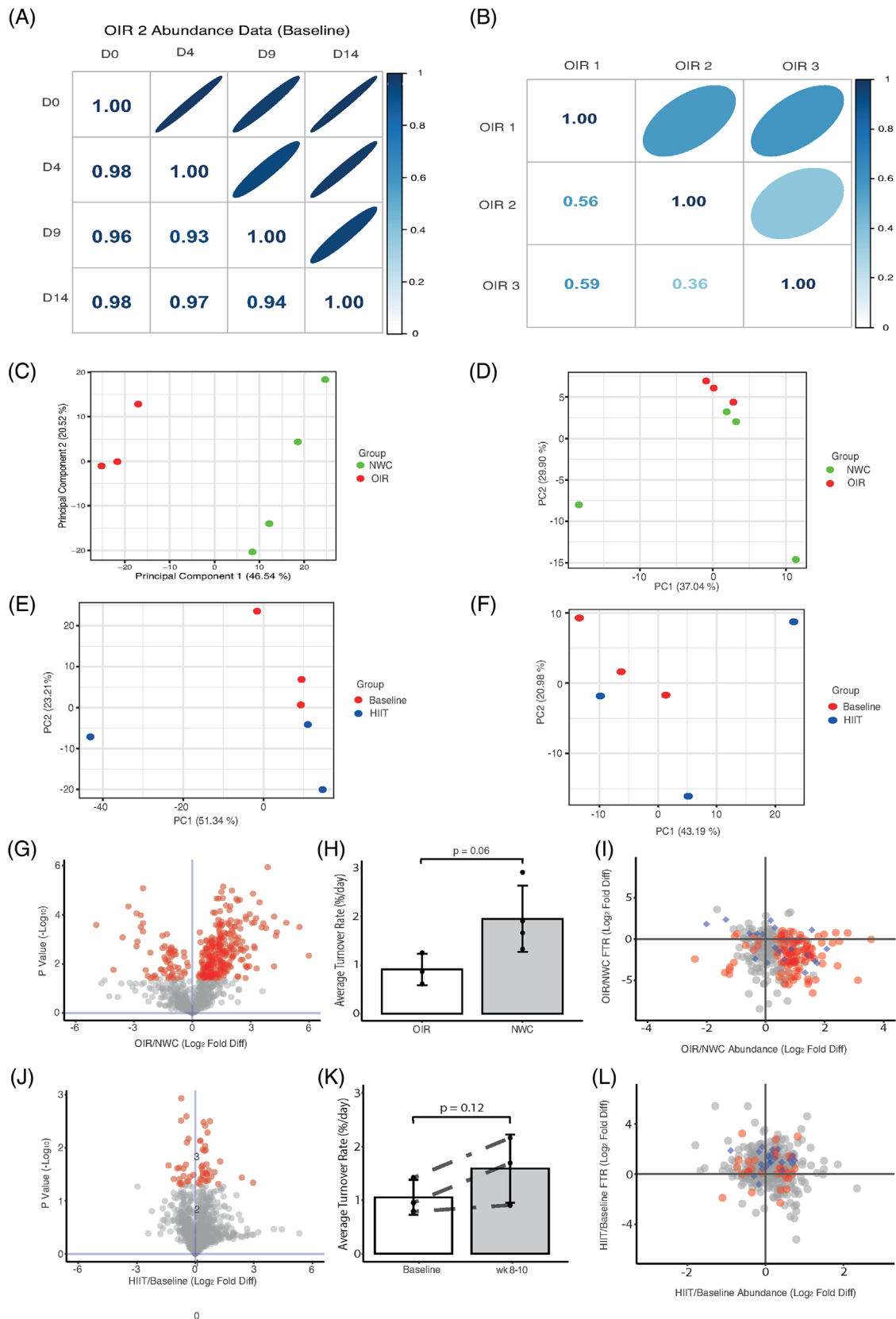


FIGURE 2 Dynamic proteome profiling of human muscle. (A) Correlation matrix illustrating the technical reproducibility of muscle protein abundance data ($n = 919$ proteins quantified) from a participant sampled at days 0, 4, 9, and 14 of the baseline experimental period. (B) Correlation matrix illustrating the biological variation of protein fractional turnover rates ($n = 378$ proteins) quantified in $n = 3$ OIR participants during baseline experimental period. Principal component analysis illustrating differentiation in OIR and NWC participants based on protein abundance

TABLE 1 Physical and physiological characteristics measured during pre- and post-experimental testing of the normal-weight healthy control (NWC) and obese insulin resistant (OIR) individuals at baseline and after 10-weeks HIIT exercise. Data presented as mean \pm standard deviation.

* $p < 0.05$; ** $p < 0.01$; # $p < 0.1$ versus OIR baseline.

	NWC ($n = 4$)	OIR (Baseline) ($n = 3$)	OIR (Post-exercise) ($n = 3$)
Age (Years)	38 \pm 8	38 \pm 6	
Height (cm)	177.1 \pm 5.9	179.7 \pm 4.1	
Weight (kg)	75.6 \pm 5.1	113 \pm 25	112 \pm 27
BMI (kg m ²)	24.2 \pm 2.4*	34.0 \pm 5.8	34.8 \pm 6.1
Fat mass (kg)	13.5 \pm 3.9*	32.9 \pm 14.11	32.4 \pm 14.0
Fat free mass (kg)	55.9 \pm 3.0**	70.3 \pm 5.7	70.6 \pm 7.5
Percent body fat (%)	18.3 \pm 4.3*	30.2 \pm 7.5	30.1 \pm 6.4
VO _{2peak} (mL kg ⁻¹ min ⁻¹)	45.5 \pm 7.9**	26.2 \pm 4.4	28.6 \pm 7.0
VO _{2peak} (mL kg FFM ⁻¹ min ⁻¹)	61.30 \pm 9.2**	38.8 \pm 2.0	41.8 \pm 7.6
Watt _{max} (W)	259.8 \pm 48.3*	185.3 \pm 26.0	210.3 \pm 22.5#
Watt _{max} (W kg FFM ⁻¹)	4.65 \pm 0.87**	2.47 \pm 0.27	2.89 \pm 0.56
Exercise test duration (min)	19.2 \pm 3*	13.5 \pm 2.3	15.6 \pm 2
Fasting glucose (mmol l ⁻¹)	5.0 \pm 0.3	5.0 \pm 1.6	5.4 \pm 0.4
Glucose AUC (mmol l ⁻¹)	703.3 \pm 81.5	849.3 \pm 441.4	739.0 \pm 298.8
Fasting insulin (uIU mL ⁻¹)	8.6 \pm 2.9#	36.8 \pm 28.6	31.5 \pm 26.9
Insulin AUC (uIU mL ⁻¹)	5422 \pm 2627#	9292 \pm 172	15058 \pm 8023
Matsuda Index	5.7 \pm 1.4*	1.9 \pm 0.7	2.1 \pm 1

Note. Physical and physiological characteristics measured during pre- and post-experimental testing of the normal-weight healthy control (NWC) and obese insulin resistant (OIR) individuals at baseline and after 10-weeks HIIT exercise. Data presented as mean \pm standard deviation. * $p < 0.05$; ** $p < 0.01$; # $p < 0.1$ versus OIR baseline.

proteins that decreased in response to the HIIT intervention (Figure 2I, Table S2).

Protein turnover rates were measured for 378 proteins that had high-quality peptide mass isotopomer data matched between $n = 3$ participants in the OIR and NWC groups at baseline or 409 proteins matched within the $n = 3$ OIR participants at baseline and after the HIIT intervention. Protein-specific turnover values were aggregated to derive the average rate of turnover (%/d) of mixed protein (Table S3), which tended ($p = 0.061$) to be greater in NWC (1.95 ± 0.68) than OIR (0.91 ± 0.32) muscle at baseline (Figure 2H) and increased 1.5-fold ($p = 0.12$) to $1.59 \pm 0.63\%$ /d in OIR muscle during weeks 8–10 of HIIT (Figure 2K).

Nineteen individual proteins exhibited differences ($p < 0.05$) in turnover rate at baseline (Figure 2J, Table S4), including 11 greater

in NWC and 8 greater in OIR. Seven proteins were significantly more abundant in OIR muscle, but their turnover rate was significantly less than in NWC muscle. In addition, 10 proteins exhibited significant differences in the turnover rate but were not different in abundance between OIR and NWC groups (Figure 2L). There were significant ($p < 0.05$) changes in the turnover of 22 individual proteins between baseline and the final 2-weeks of training (Figure 2J, Table S5). Twenty-one proteins changed in turnover independent of changes in protein abundance (19 increasing, 2 decreasing in turnover rate). Whereas only 1 protein, 14-3-3 protein Epsilon (14-3-3E), increased in abundance and turnover rate in response to the HIIT.

Proteins that exhibited significant differences between NWC and OIR baseline or changes in OIR from pre- to post- HIIT were enriched for KEGG pathways relating to energy metabolism (Figure 3),

profile (C) or fractional turnover rates (D). Principal component analysis illustrating differentiation in OIR at baseline and after 10-weeks of high intensity interval training (HIIT) participants based on protein abundance profile (E) and fractional turnover rates (F). (G) Volcano plot illustrating Log2 fold-difference in protein abundance between OIR and NWC muscle at baseline. Statistically significant ($p < 0.05$) data with a false discovery rate (FDR) $< 5\%$ are highlighted in red. (H) Average turnover rate of proteins ($n = 378$) quantified in OIR ($n = 3$) and NWC ($n = 4$) participants during the baseline measurement period. (I) Scatter plot of co-occurring differences (Log2 transformed data) in protein abundance (x-axis) and turnover rate (y-axis) in OIR compared to NWC participants. (J) Volcano plot illustrating Log2 fold-change in protein abundance in OIR participants between baseline (day 0) and the end (day 14) of the HIIT intervention. Statistically significant ($p < 0.05$) data are highlighted in red, the FDR threshold for this data is $> 40\%$. (K) Average turnover rate of proteins ($n = 409$) quantified in OIR ($n = 3$) during the baseline measurement period and final 2-weeks of the HIIT intervention. (L) Scatter plot of co-occurring changes (Log2 transformed data) in protein abundance (x-axis) and turnover rate (y-axis) in OIR participants after the HIIT intervention.

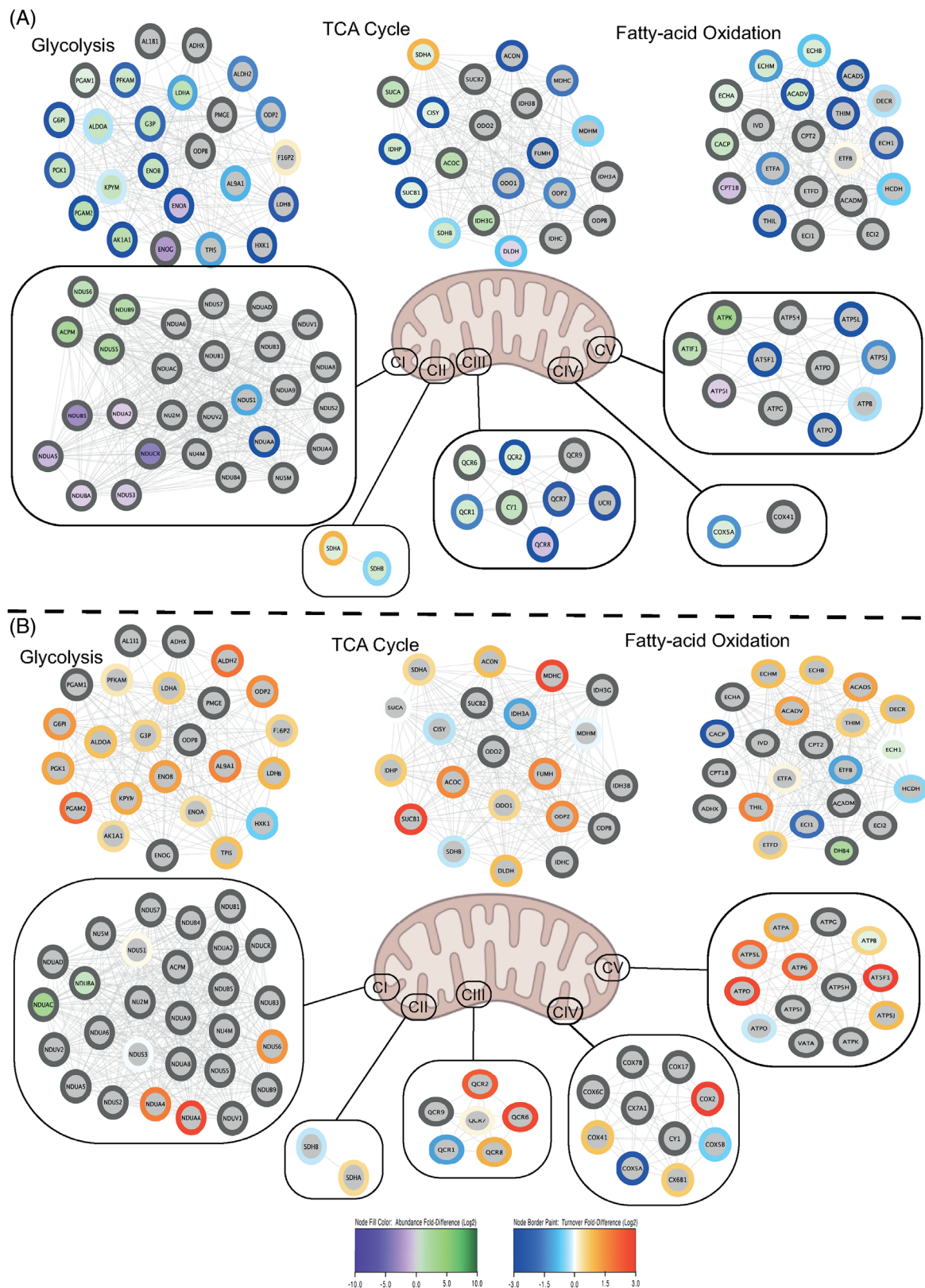


FIGURE 3 Dynamic proteome profiling of muscle energy metabolism pathways. Nodes represent proteins organized to their principal energy metabolism pathway in muscle and are annotated by their UniProt knowledgebase identifier. (A) Node fill colour represents Log2 fold-difference in abundance and node boarder colour represents Log2 fold-difference in fractional turnover rate (FSR) between obese-insulin resistant (OIR) and normal-weight healthy control (NWC) participants at baseline. (B) Node fill colour represents Log2 fold-change in abundance and node boarder colour represents Log2 fold-chance in fractional synthesis rate in obese-insulin resistant (OIR) after the 10-week high-intensity interval training (HIIT) intervention. Grey borders indicate missing FSR data. CI–CV represent mitochondrial respiratory chain complexes.

proteasome and cell stress (Figure 4), and the patterns of proteodynamics for each of these biological collections is presented below.

3.3 | Proteodynamic analysis of proteins associated with muscle energy metabolism pathways

Thirteen proteins associated with glycolysis/gluconeogenesis (of 24 quantified) were significantly different in abundance between OIR and NWC groups. The majority (11 proteins) of glycolytic proteins were more abundant in OIR muscle. Turnover rates were measured for 17 glycolytic/gluconeogenic enzymes and the turnover of each protein tended to be less in OIR than NWC muscle (Figure 3A). In response to HIIT, two proteins associated with glycolytic metabolism (glycerol-3-phosphate phosphatase; PGP) and glycogen phosphorylase; PYGM) increased ~1.2-fold in abundance ($p = 0.038$ and 0.030 , respectively). Similarly, peroxisomal multifunctional enzyme 2 (DHB4) exhibited a robust increase (~5-fold; $p = 0.036$) in abundance after HIIT (Pre = 4.478 ± 1.408 , Post = 23.338 ± 5.469 fmol/ μ g). The turnover rate of triosephosphate isomerase increased ($p = 0.046$) from $0.26 \pm 0.25\%/d$ at baseline to $0.45 \pm 0.31\%/d$ in trained OIR muscle and the turnover of phosphoglucomutase-1 (PGM1) increased ~3-fold ($p = 0.011$) between baseline ($0.34 \pm 0.36\%/d$) and the final 2-weeks of exercise ($0.92 \pm 0.46\%/d$). In each case, the increases in protein turnover rate were not associated with differences in the abundance of these proteins between baseline and HIIT conditions (Figure 3B).

Significant differences were detected amongst six enzymes (of 20 quantified) involved in fatty acid oxidation (FAO) and nine enzymes (of 21 quantified) of the tricarboxylic acid (TCA) cycle. Most enzymes associated with FAO and TCA cycle were more abundant in OIR muscle (5/6 and 8/9, respectively), whereas dihydrolipoamide dehydrogenase (DLD) was significantly greater in abundance in NWC muscle. Similar to the pattern exhibited by enzymes of glycolytic metabolism, the turnover of the FAO enzymes was generally lower in OIR muscle (Figure 3A). For example, the turnover of enoyl-CoA hydratase (ECHM), was 2.4-fold slower ($p = 0.044$) in OIR ($0.60 \pm 0.42\%/d$) compared to NWC ($1.41 \pm 0.23\%/d$) and ECHM abundance was 1.8-fold greater ($p = 0.01$, $q = 0.02$) in OIR muscle. The rate limiting enzyme of vitamin B6 metabolism, pyridoxine-5'-phosphate oxidase (PNPO), was 2.5-fold more abundant but had a 16-fold lower turnover rate in OIR ($0.24 \pm 0.41\%/d$) compared to NWC ($4.04 \pm 2.07\%/d$) muscle. The redox enzyme, dehydrogenase/reductase SDR family member 7 (DHRS7), was 4-fold more abundant ($p = 0.005$, $q = 0.01$) but had a 2.3-fold ($p = 0.015$) slower turnover rate in OIR compared to NWC muscle at baseline. Exercise led to changes in the abundance or turnover rate of several proteins associated with metabolic pathways (Figure 3B). Long-chain fatty acid CoA ligase-1 (ACSL1) and delta(3,5)-delta(2,4)-dienoyl-CoA isomerase, mitochondrial (ECH1) increased in abundance ~1.6 fold ($p = 0.03$ and $p = 0.27$, respectively). Whilst short-chain specific acyl-CoA dehydrogenase (ACADS) did not change in abundance,

ACADS increased ($p = 0.024$) 2.4-fold in turnover rate in response to exercise training.

3.4 | Proteodynamic analysis of respiratory chain subunits

Twenty-four proteins (of 61 quantified) belonging to the KEGG pathway "oxidative phosphorylation" (OXPHOS) exhibited significant differences in abundance between OIR and NWC groups (Figure 3A). NADH dehydrogenase (Complex I) exhibited the greatest number of differences and 10 subunits (of 28 quantified) exhibited significant differences in abundance between OIR and NWC groups. Six proteins (NDUB5, NDUS3, NDUCR, NDUA2, NDUA5, and NDUBA) were less abundant and four subunits (NDUB9, NDUS6, NDUS5, and ACPM) were more abundant in OIR muscle. Subunits A and B of succinate dehydrogenase (SDH; Complex II) were significantly ($p < 0.05$, FDR < 5%) more abundant in OIR muscle compared to NWC, but there was no difference in abundance of the two membrane-anchoring SDH subunits, C and D. Eight subunits of Complex III (Cytochrome c reductase) were quantified and five exhibited significant differences between OIR and NWC participants. Cytochrome c (CY1) and two other core subunits of the cytochrome b-c1 complex (QCR1 and QCR2) were significantly more abundant in OIR as was subunit 6 (QCR6) which is associated with the low molecular weight component of Complex III. Subunit 8 (QCR8), which is also associated with the low molecular weight sub-complex, was significantly less abundant in OIR muscle. Cytochrome c oxidase subunit 5A (COX5A) was the only subunit of seven quantified from Complex IV that was significantly less abundant ($p = 0.03$, $q = 0.04$) in OIR muscle. Eleven subunits of ATP synthase (Complex V) were analysed, and three exhibited significant differences in abundance between NWC and OIR muscle. ATP synthase subunits f (ATPK) and the endogenous inhibitor (ATIF1) were more abundant (8.4-fold and 2.9-fold, respectively), in OIR muscle. Conversely, ATP5I was more abundant in NWC muscle and (1.8-fold). Alongside protein abundance profiling our analysis quantified the turnover rates of 15 OXPHOS subunits. Generally, the turnover data indicated a theme of lower mean turnover rate in OIR muscle (Figure 3) and the rate of turnover of 1 protein, Cytochrome b-c1 complex subunit Rieske (UCRI), was statistically ($p = 0.025$) greater in NWC ($2.78 \pm 1.20\%/d$) compared to OIR ($0.37 \pm 0.55\%/d$) muscle.

Two subunits of respiratory Complex I, including alpha-subcomplex 12 (NDUAC) and beta subcomplex subunit 10 (NDUBA) that were significantly less abundant in OIR compared to NWC at baseline, increased in abundance by 2.4-fold ($p = 0.018$) and 7.8-fold ($p = 0.045$), respectively after HIIT (Figure 3B). ATP synthase subunit beta (ATPB) increased (1.3-fold, $p = 0.04$) from 32.73 ± 9.94 fmol/ μ g at baseline to 42.27 fmol/ μ g post-HIIT. Two other ATP synthase subunits (G; ATP5L and A; ATPA) exhibited greater turnover rates after 10 weeks HIIT but their abundance was unaffected. ATP5L exhibited a robust increase (~4-fold, $p = 0.007$) in turnover rate from $0.21 \pm 0.34\%/d$ at baseline to $0.82 \pm 0.36\%/d$ across the final 2-weeks of exercise. ATPA

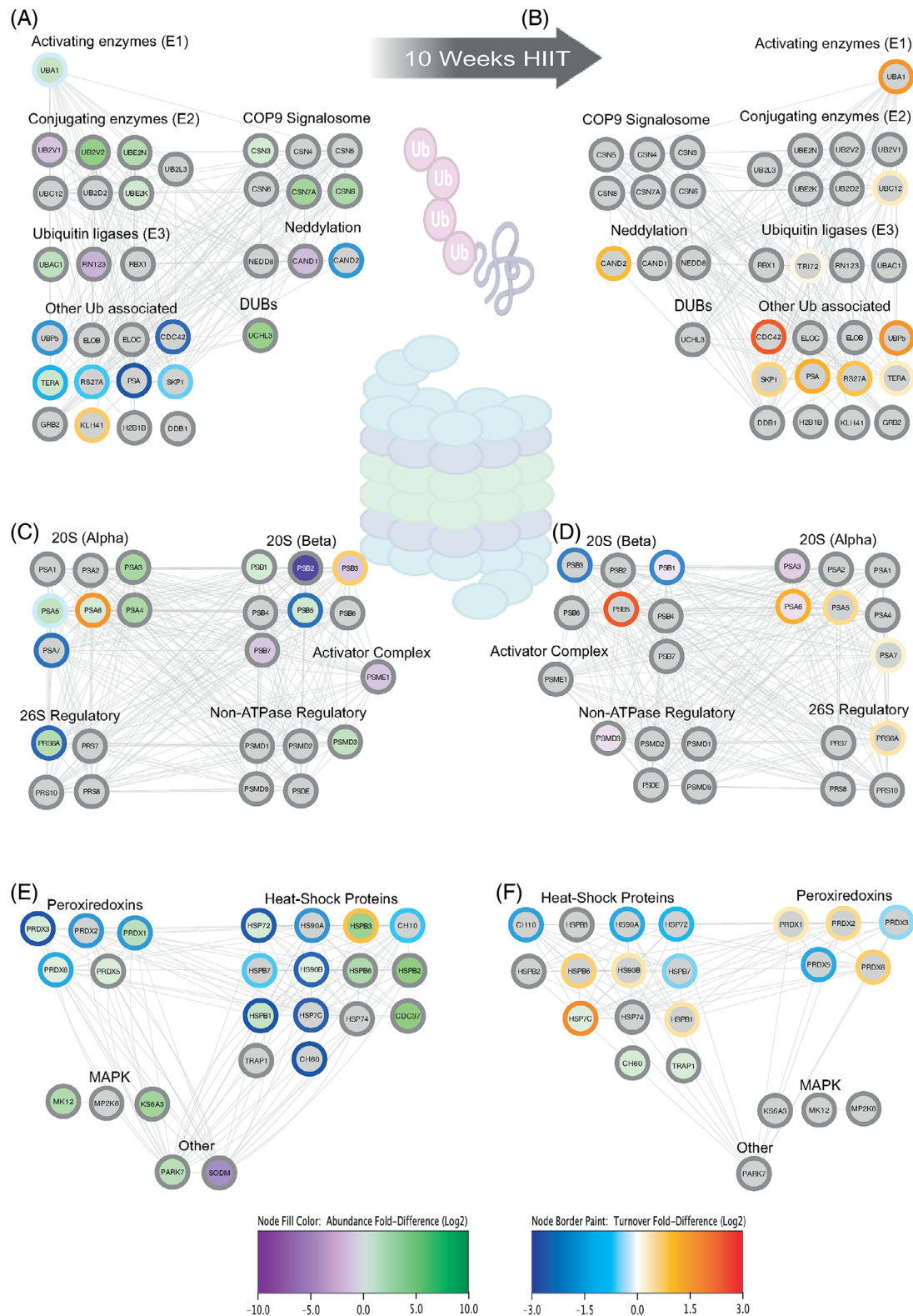


FIGURE 4 Dynamic proteome profiling of the muscle proteostasis network. Nodes represent proteins annotated by their UniProt knowledgebase identifier and organized to their principal proteostasis network components, including ubiquitin ligase (A and B), proteasome (C and D) or heat shock protein and antioxidant system (E and F). (A, C, and E) Node fill colour represents Log2 fold-difference in abundance and node boarder colour represents Log2 fold-difference in fractional synthesis rate (FSR) between obese-insulin resistant (OIR) and normal-weight healthy control (NWC) participants at baseline. (B, D, and F) Node fill colour represents Log2 fold-change in abundance and node boarder colour represents Log2 fold-change in fractional turnover rate in obese-insulin resistant (OIR) after the 10-week high-intensity interval training (HIIT) intervention. Grey borders indicate missing FSR data.

increased > 2-fold ($p = 0.045$) in turnover rate in response to training in OIR muscle.

3.5 | Proteodynamic analysis of proteins associated with the proteasome, ubiquitination, or cellular stress response

Proteins belonging to the KEGG "Proteasome" pathway were highly enriched ($q = 5.3e^{-4}$) amongst the significant differences between OIR and NWC muscle. Several enzymes involved in protein ubiquitination exhibited significantly greater abundance in OIR muscle (Figure 4), including the E1 enzyme, ubiquitin-like modifier-activating enzyme 1 (UBA1), E2 ubiquitin-conjugating enzymes UBE2N, UBE2K, UB2V2, and the E3 ligases, UBAC1 and TRI72. There were some exceptions to this pattern, for example variant 1 of the E2 enzyme, UB2V1, was ~2-fold greater ($p = 0.003$, $q = 0.009$) in NWC muscle and the abundance of the E3 ligase RNF123, was ~3-fold greater ($p = 0.002$, $q = 0.008$) in NWC. Two subunits of the COP9 signalosome (a deactivator of Cullin-RING ubiquitin ligases) were more abundant in OIR muscle, and a protein involved in mitophagy, FUN14 domain-containing protein 2, was ~9-fold greater in abundance in OIR (0.3407 ± 0.0920 fmol/ μ g) than NWC (0.0374 ± 0.0424 fmol/ μ g).

Our analysis encompassed 24 of the 43 known subunits of the 26S proteasome, including all 7 alpha (PSMA) and 7 beta (PSMB) subunits that make up the 20S catalytic core, four subunits of the 19S base region (PSMC), five subunits of the 19S lid region (PSMD), and one subunit of the 11S proteasome activator (PSME). Non-ATPase regulatory subunit 3 (PSMD3) and proteasome regulatory subunit 6A (PRS6A) were significantly more abundant in OIR muscle, alongside greater abundances of alpha subunits 3, 4, 5, and 6, and beta subunits 1 and 5, of the core particle (Figure 4C). Conversely beta subunits 2, 3, and 7, and the proteasome activator complex subunit 1 (PSME1) were significantly more abundant in NWC muscle. Protein turnover rates were quantified for 6 proteasome subunits but no statistically significant differences in turnover were identified between OIR and NWC groups.

Fifteen proteins associated with response to stress and chaperone function differed in abundance between OIR and NWC muscle, including four isoforms of peroxiredoxin (PRDX), each more abundant in OIR than NWC muscle (Figure 4E). PRDX1 exhibited the greatest difference and was ~2.5-fold greater ($p = 0.008$, $q = 0.02$) in OIR muscle. Similarly, PRDX3, PRDX5, and PRDX6 were each ~1.5-fold more abundant in OIR muscle. Parkinson disease protein 7 (PARK7) was 2.5-fold greater ($p < 0.001$, $q = 0.001$) in abundance in OIR muscle (26.89 ± 0.22 fmol/ μ g) than NWC (10.54 ± 1.80 fmol/ μ g), whereas the mitochondrial superoxide scavenging enzyme, superoxide dismutase (SODM) was greater ($p < 0.001$, $q = 0.003$) in abundance in NWC (1.965 ± 0.300 fmol/ μ g) than OIR muscle (0.3132 ± 0.1259 fmol/ μ g).

Several proteins associated with maintaining proteostasis were more abundant but had a slower turnover rate in OIR muscle. Heat-shock 70 kDa protein 1 (HSP72) exhibited a 5-fold slower turnover ($p = 0.01$) in OIR (0.74 ± 0.56 %/d) compared to NWC muscle (4.11 ± 1.14 %/d) whilst being ~1.5-fold more abundant ($P = 0.017$,

$q = 0.028$) in OIR. Similarly, the detoxifying enzyme (aldo-keto reductase, mitochondrial; AK1A1) exhibited a 3-fold greater abundance in OIR muscle but turned over at a rate of 1.11 ± 0.31 %/d in OIR and 8.50 ± 1.18 %/d in NWC muscle (7-fold slower in OIR; $p < 0.001$). Mitochondrial aldehyde dehydrogenase 2 (ALDH2) is a second enzyme associated with alcohol metabolism and protects against oxidative stress. ALDH2 had a significantly greater turnover rate in endurance trained muscle (4.12 ± 1.14 %/d) compared to OIR (1.44 ± 1.18 %/d) and did not differ in abundance between groups. The plasma protein, Hemopexin (HEMO), which protects against heme-mediated oxidative stress was 3-fold greater in abundance ($p = 0.009$, $q = 0.19$) and 2-fold greater in FSR ($p = 0.011$) in OIR than NWC muscle at baseline.

After the HIIT intervention, four proteasome subunits that were more abundant in OIR muscle than NWC under baseline conditions became significantly less abundant after exercise (Figure 4D). Ten weeks of HIIT also led to robust changes in the abundance and/or turnover rates of proteins associated with chaperone functions (Figure 4F). The abundance of the mitochondrial heat shock protein, HSP 75 kDa (TRAP1), increased 1.5-fold ($p = 0.021$) from 0.096 ± 0.030 fmol/ μ g at baseline to 0.143 ± 0.026 fmol/ μ g after 10 weeks HIIT. Similarly, chaperonin 60 (CH60) exhibited a 1.6-fold increase ($p = 0.041$) in abundance after the HIIT intervention from 2.790 ± 0.190 fmol/ μ g at baseline to 4.431 ± 0.665 fmol/ μ g post-training. The adapter protein 14-3-3E, which may positively regulate the heat shock response increased in abundance from 8.178 ± 1.891 fmol/ μ g to 9.029 ± 2.218 fmol/ μ g post-exercise ($p = 0.046$). Notably, the abundance of the chaperone, heat shock cognate 71 kDa (HSP7C) increased 1.4-fold ($p = 0.042$) after HIIT specifically in the myofibrillar fraction. The abundance of HSP7C within the soluble fraction remained stable between pre- and post-exercise in OIR muscle, whereas HSP7C turnover increased 2.7-fold ($p = 0.004$). The chaperone HS90-beta also significantly increased in turnover rate ($p = 0.046$) between baseline (4.46 ± 1.07 %/d) and in response to exercise (5.74 ± 1.23 %/d). In addition, exercise training increased the turnover rates of PRDX2 and ALDH2, which exhibited a significantly greater FSR ($p = 0.050$ and 0.037 , respectively) in trained OIR muscle (0.58 ± 0.25 and 5.58 ± 1.87 %/d, respectively) in comparison to baseline (0.43 ± 0.26 and 1.44 ± 1.18 %/d) (Figure 4F).

4 | DISCUSSION

Proteostasis describes the maintenance of proteome quality and encompasses the processes of protein turnover and the actions of chaperone systems that safeguard proteins during discrete stages of their lifecycle. Our current findings point to dysregulation of proteostasis in OIR individuals, while longitudinal analysis of OIR muscle after a 10-week programme of HIIT revealed some restoration of muscle proteostasis. During their lifecycle, proteins accumulate damage through irreversible spontaneous modifications (e.g., deamination) in a time-dependent manner [15]. Deamination caused by nucleophilic attack may particularly occur during the catalytic cycle of enzymes [16] and turnover is required to maintain the quality of the enzyme pool.

We report glycolytic enzymes were more abundant but had slower rates of turnover in OIR muscle at baseline (Figure 3), which may indicate a poorer protein quality compared to NWC muscle. In model systems, the catalytic activity of metabolic enzymes is positively correlated with their turnover rate [17]. Therefore, the lesser turnover of glycolytic enzymes in OIR muscle agrees with the lower rates of glucose utilisation reported [18] in the muscle of people with obesity. However, this accumulation of glycolytic enzymes with suboptimal rates of turnover may burden protein quality control systems responsible for the removal of damaged proteins. Indeed, the fundamental components of the proteostasis network, including the ubiquitin proteasome system (UPS) and heat-shock protein (HSP) chaperones, featured prominently amongst the differences between OIR and NWC muscle proteomes.

E3 ubiquitin ligases underpin the selectivity of UPS-mediated protein degradation and have been a focus of mechanistic studies. The E3 ubiquitin ligase, tripartite motif-containing protein 72 (TRIM72), was more abundant and had a lower turnover rate in OIR muscle. TRIM72 ubiquitinates the insulin receptor and insulin receptor substrate-1 (IRS1) and negatively affects muscle insulin signalling [19]. Consistent with our findings, muscle TRIM72 abundance is greater in models of obesity and insulin resistance, whereas knock-down of TRIM72 protects against muscle insulin resistance induced by a high-fat diet [20]. HIIT did not alter TRIM72 abundance but did significantly increase TRIM72 turnover, which may be an early indication of a beneficial effect of HIIT. OIR muscle also exhibited differences in the Cop9 signalosome, which regulates the large family of cullin-RING ubiquitin E3 ligases (CRL) by removing the nedd8 ubiquitin-like modifier from cullin subunits. Only Nedd8-modified CRL complexes are catalytically active and two subunits of the COP9 signalosome (CSN3 and CSN7A) were more abundant in OIR muscle at baseline (Figure 4), which may indicate lesser activation of CRL enzymes. Cullin-associated NEDD8-dissociated protein 2 (CAND2) is also specific to striated muscle and suppresses the activity of SCF (Skp1-Cullin1-F-box protein)-like ubiquitin E3 ligase complexes by binding culin1 to prevent neddylation [21]. No difference in CAND2 abundance was detected, but the turnover of CAND2 was less in OIR compared to NWC at baseline and increased in OIR muscle after exercise training. In addition, the deubiquitinating enzyme, ubiquitin carboxyl-terminal hydrolase isozyme L3 (UCHL3), which hydrolyses the peptide bond of both ubiquitin and nedd8 modifications [22], was significantly more abundant in OIR muscle. Together these findings indicate disruption to nedd8 post-translational modifications that regulate the activity of key E3 ligase families in muscle.

Ubiquitin E2 enzymes (UBE2- N, K, V1, and V2) also exhibited different abundances between OIR and NWC muscle, particularly those associated with the regulation of K⁶³-polyubiquitination. Ubiquitin-conjugating enzyme E2 N (UBE2N) forms heterodimers with either UBE2 variant 1 (UBE2V1) or UBE2 variant 2 (UBE2V2) and regulates the assembly of K⁶³-polyubiquitin chains; whereas UBE2K is responsible for generating branched chains containing both k⁴⁸- and k⁶³-linked ubiquitins. Polyubiquitin chains joined at ubiquitin K⁴⁸ are an acknowledged degradative signal, whereas the inclusion of K⁶³ linkages may

counter the signal for proteasomal degradation [23]. The UBE2N/V2 heterodimer (each more abundant in OIR muscle) is associated with protection against DNA damage [24] whereas only UBE2V1 isoform was enriched in NWC muscle. UBE2V1 modulates ubiquitin proteasome responses to proteotoxic stress [25] and the greater likelihood of UBE2N/UBE2V1 heterodimers in NWC muscle may be associated with superior proteostasis. Conversely, UBE2V2 can be modified by reactive electrophiles and may lead to hyperactivation of UBE2N to promote K⁶³-polyubiquitination and genome protection [26]. UBE2K was also significantly more abundant in OIR muscle and is responsible for the formation of branched polyubiquitin chains that contain K⁴⁸- as well as K⁶³-linkages [27]. UBE2K may enhance proteasomal degradation of proteins carrying K⁶³-polyubiquitin chains [28]. These findings highlight a complex interplay between E2 ligases and suggest the distribution of K⁴⁸- and K⁶³-linked polyubiquitin chains was altered in the muscle of OIR participants.

The catalytically active subunits of the core proteasome (beta 1, 2, and 5) differed in abundance between OIR and NWC muscle. The beta-1 and beta-5 subunits were significantly more abundant in OIR muscle, whereas the beta-2 subunit was significantly less abundant compared to NWC muscle. Previous studies [29, 10] similarly report some but not all proteasome subunits exhibit differences amongst the muscle of people with and without obesity. Proteasome activity is also modified by changes to regulatory subunits, including the 11S proteasome activator (PA28 α ; PSME1), which increases specifically in the muscle of people with obesity after acute exercise [10]. Similarly, we found PSME1 was more abundant in OIR muscle after 10-weeks HIIT (Figure 4D) and our earlier analysis of responses to exercise in rat heart [30] also found endurance training increases the abundance of the PSME1 subunit. Overexpression of PSME1 is associated with increased degradation of oxidatively damaged proteins in rat neonatal ventricular myocytes [31]. Whereas streptozotocin-induced insulin-dependent diabetes is associated with reduced muscle PSME1 content and loss of proteasome activity [32]. Therefore, despite ambiguous differences in catalytically active subunits of the core proteasome, 10-weeks HIIT may have improved the capacity for proteasomal degradation in the muscle of OIR participants via 11S proteasome activation.

HSP are major constituents of the proteostasis network and are categorized into major families (e.g., 90 kDa-, 70 kDa-, and small (< 45 kDa) heat-shock proteins) by their molecular weight. Small HSP (sHSP) function in homo- or hetero-oligomers of various sizes and complexity and the observed differences across several sHSP (Figure 4E) may indicate changes to the size or composition of sHSP oligomers. sHSP bind efficiently with misfolded proteins but lack ATPase activity and cannot (re-) fold substrate proteins directly [33] so work cooperatively with other chaperone complexes, for example, by preparing proteins for refolding by HSP70 [34]. The inducible HSP72 and the constitutively expressed heat shock cognate (HSP7C) were each more abundant in OIR than NWC muscle. Chronic elevation of HSP72 in OIR muscle may be evidence of sustained stress and an elevated requirement for refolding damaged proteins [35]. Indeed, muscle-specific overexpression of HSP72 can protect against the development of insulin resistance induced by a high-fat diet in mice [36]. Herein, HIIT did

not affect HSP72 but did significantly increase the turnover rate of HSP7C, which may support an improvement in proteome quality by enhancing the capability of HSP7C to orchestrate chaperone-mediated degradative process [37].

HSP70 complexes may, in turn, pass client proteins to HSP90 complexes, including HSP90- α (HS90A) and HSP90- β (HS90B), which are abundant cytosolic proteins that (re-) fold newly synthesized or incorrectly folded protein clients. Pharmacological inhibition [38] or knockdown [39] of HSP90 improves insulin sensitivity in rodent models of diabetes or diet-induced obesity. Consistent with findings in patients with type 2 diabetes [40], HSP90B was more abundant in OIR muscle (Figure 4E). HIIT did not alter the abundance of either HSP90 isoform but the turnover rate HS90B increased significantly in OIR muscle after 10-weeks of training (Figure 4F). HSP90 function is regulated by post-translational modifications, including oxidation [41], and a greater turnover of HSP90 in trained muscle may equate to a greater proportion of non-modified HSP90 proteins, which have preserved functional capacity [42]. In addition, the mitochondrially targeted homolog of HSP90, TRAP1, was more abundant in OIR muscle after HIIT, and TRAP1 may offer greater protection against mitochondrial apoptosis induced by reactive oxygen species [43].

Redox signalling contributes to the muscle response to exercise, and oxidative stress is a proposed mechanism of muscle dysfunction associated with obesity. PARK7 (DJ-1) and peroxiredoxins (PRDX) were generally more abundant in OIR than NWC muscle. PARK7 is a redox-sensitive chaperone that may reverse methylglyoxal and glyoxal-glycated protein modifications [44] that can be elevated in the muscle of people with obesity or type 2 diabetes [45]. PRDX enzymes are the primary scavengers of cellular H_2O_2 and may underpin the hormesis response of muscle to exercise-induced oxidative stress [46]. Our findings (Figure 4E and F) add to reports that PRDX2 and PRDX6 are more abundant in the skeletal muscle of patients with type 2 diabetes [47], and that PRDX5 is more abundant in myoblasts derived from muscle biopsies of type 2 diabetic patients [48].

Our protein-by-protein analysis of abundance and turnover responses has yielded new insight into losses in muscle proteostasis associated with obesity. Our findings are based on highly stringent data handling, including critical analysis of the alignment of LC-MS peptide retention patterns and the exclusion, rather than imputation, of peptides with missing data. During each measurement period, a time series of $n = 4$ samples was collected from each participant to determine the turnover rate and abundance of each protein in each experimental condition. Our statistical analyses of protein-level data were conducted using only those proteins that are detected in each participant at every timepoint, which is crucial in within-subject repeated measures designs. We acknowledge our sample size of $n = 4$ NWC and $n = 3$ OIR participants limits the extrapolation of our findings to larger populations. More extensive studies are required to pursue this line of enquiry in the future and power analyses [11] suggest $n > 12$ may be required. Nevertheless, our current early findings offer new insight and align well with existing protein abundance profiling studies (reviewed in [8]) and the limited available data on protein-specific synthesis in the muscle of people with obesity. For instance, Tran et al., [49]

used targeted analysis of ATP synthase beta (ATPB) in $^2H_{10}$ -leucine labelled samples to report a lesser turnover of ATPB in the muscle of people with obesity. We also found ATPB turnover was less in OIR muscle, in addition, our analysis encompassed a further 10 subunits of Complex V and highlighted that subunits AT5F1, ATP5L, and ATPO also exhibited lesser rates of turnover in OIR muscle (Figure 3A).

In conclusion, the muscle proteome of people with obesity exhibits widespread evidence of losses in proteostasis and elevated proteome stress. Ten-weeks of HIIT tended to improve the quality of the proteome by altering proteasome composition and enhancing the turnover rates of metabolic enzymes. Losses in proteostasis are well-established in age-related diseases, and our current discoveries highlight a need to further investigate whether losses in proteostasis also underpin earlier pre-clinical stages of disease in younger adults.

ACKNOWLEDGMENTS

This work was funded by the Royal Thai Government (Strategic Plan and Policy Scholarship) and the Department of Disease Control, Ministry of Public Health, Thailand.

CONFLICT OF INTEREST STATEMENT

The authors have no conflicts of interest to declare.

DATA AVAILABILITY STATEMENT

The mass spectrometry proteomics data generated in this study have been deposited to the ProteomeXchange Consortium via the PRIDE converter tool [50] under the dataset identifier PXD043020, project <https://doi.org/10.6019/PXD043020>.

ORCID

Jatin G. Burniston  <https://orcid.org/0000-0001-7303-9318>

REFERENCES

- Kolb, H., Kempf, K., Röhling, M., & Martin, S. (2020). Insulin: Too much of a good thing is bad. *BMC medicine*, 18(1), 224–224. <https://doi.org/10.1186/s12916-020-01688-6>
- Freitas, E. D. S., & Katsanos, C. S. (2022). (Dys)regulation of protein metabolism in skeletal muscle of humans with obesity. *Frontiers in Physiology*, 13, 843087. <https://doi.org/10.3389/fphys.2022.843087>
- Qi, Y., Zhang, X., Seyoum, B., Msallaty, Z., Mallisho, A., Caruso, M., Damacharla, D., Ma, D., Al-Janabi, W., Tagett, R., Alharbi, M., Calme, G., Mestareehi, A., Draghici, S., Abou-Samra, A., Kowluru, A., & Yi, Z. (2020). Kinome profiling reveals abnormal activity of kinases in skeletal muscle from adults with obesity and insulin resistance. *Journal of Clinical Endocrinology and Metabolism*, 644(3). <https://doi.org/10.1210/clinem/dgz115>
- Tran, L., Hanavan, P. D., Campbell, L. E., De Filippis, E., Lake, D. F., Coletta, D. K., Roust, L. R., Mandarino, L. J., Carroll, C. C., & Katsanos, C. S. (2016). Prolonged exposure of primary human muscle cells to plasma fatty acids associated with obese phenotype induces persistent suppression of muscle mitochondrial ATP synthase β subunit. *PLoS ONE*, 11(8), e0160057. <https://doi.org/10.1371/journal.pone.0160057>
- Tran, L., Kras, K. A., Hoffman, N., Ravichandran, J., Dickinson, J. M., D'Iugos, A., Carroll, C. C., Patel, S. H., Mandarino, L. J., Roust, L., & Katsanos, C. S. (2018). Lower fasted-state but greater increase in muscle protein synthesis in response to elevated plasma amino acids in

- obesity. *Obesity (Silver Spring)*, 26(7), 1179–1187. <https://doi.org/10.1002/oby.22213>
6. Guillet, C., Delcourt, I., Rance, M., Giraudet, C., Walrand, S., Bedu, M., Duche, P., & Boirie, Y. (2009). Changes in basal and insulin and amino acid response of whole body and skeletal muscle proteins in obese men. *Journal of Clinical Endocrinology and Metabolism*, 94(8), 3044–3050. <https://doi.org/10.1210/jc.2008-2216>
 7. Beals, J. W., Sukienik, R. A., Nallabelli, J., Emmons, R. S., Van Vliet, S., Young, J. R., Ulanov, A. V., Li, Z., Paluska, S. A., De Lisio, M., & Burd, N. A. (2016). Anabolic sensitivity of postprandial muscle protein synthesis to the ingestion of a protein-dense food is reduced in overweight and obese young adults. *American Journal of Clinical Nutrition*, 104(4), 1014–1022. <https://doi.org/10.3945/ajcn.116.130385>
 8. Srisawat, K., Shepherd, S., Lisboa, P., & Burniston, J. (2017). A Systematic review and meta-analysis of proteomics literature on the response of human skeletal muscle to obesity/type 2 diabetes mellitus (T2DM) versus exercise training. *Proteomes*, 5(4), 30–30. <https://doi.org/10.3390/proteomes5040030>
 9. Camera, D. M., Burniston, J. G., Pogson, M. A., Smiles, W. J., & Hawley, J. A. (2017). Dynamic proteome profiling of individual proteins in human skeletal muscle after a high-fat diet and resistance exercise. *FASEB Journal*, 31(12), 5478–5494. <https://doi.org/10.1096/fj.201700531R>
 10. Vanderboom, P., Zhang, X., Hart, C. R., Kunz, H. E., Gries, K. J., Heppelmann, C. J., Liu, Y., Dasari, S., & Lanza, I. R. (2022). Impact of obesity on the molecular response to a single bout of exercise in a preliminary human cohort. *Obesity (Silver Spring, Md.)*, 30(5), 1091–1104. <https://doi.org/10.1002/oby.23419>
 11. Srisawat, K., Hesketh, K., Cocks, M., Strauss, J., Edwards, B. J., Lisboa, P. J., Shepherd, S., & Burniston, J. G. (2019). Reliability of protein abundance and synthesis measurements in human skeletal muscle. *Proteomics*, 1900194, 1900194–1900194. <https://doi.org/10.1002/pmic.201900194>
 12. Cocks, M., Shaw, C. S., Shepherd, S. O., Fisher, J. P., Ranasinghe, A. M., Barker, T. A., Tipton, K. D., & Wagenmakers, A. J. M. (2013). Sprint interval and endurance training are equally effective in increasing muscle microvascular density and eNOS content in sedentary males. *The Journal of Physiology*, 591(3), 641–656. <https://doi.org/10.1113/jphysiol.2012.239566>
 13. Burniston, J. G. (2019). *Investigating muscle protein turnover on a protein-by-protein basis using dynamic proteome profiling*. In Burniston, J. G., & Chen, Y.-W. (Eds.) Springer, pp. 171–190. https://doi.org/10.1007/978-1-4939-9802-9_9
 14. Szklarczyk, D., Gable, A. L., Lyon, D., Junge, A., Wyder, S., Huerta-Cepas, J., Simonovic, M., Doncheva, N. T., Morris, J. H., Bork, P., Jensen, L. J., & Mering, C. V. (2019). STRING v11: Protein–protein association networks with increased coverage, supporting functional discovery in genome-wide experimental datasets. *Nucleic Acids Research*, 47(D1), D607–D613. <https://doi.org/10.1093/nar/gky1131>
 15. Robinson, N. E., & Robinson, A. B. (2001). Deamidation of human proteins. *Proceedings of the National Academy of Sciences*, 98(22), 12409–12413. <https://doi.org/10.1073/pnas.221463198>
 16. Hipkiss, A. R. (2011). Energy metabolism and ageing regulation: Metabolically driven deamidation of triosephosphate isomerase may contribute to proteostatic dysfunction. *Ageing Research Reviews*, 10(4), 498–502. <https://doi.org/10.1016/j.arr.2011.05.003>
 17. García-Aguilar, A., Martínez-Reyes, I., & Cuezva, J. M. (2019). Changes in the turnover of the cellular proteome during metabolic reprogramming: A role for mtROS in proteostasis. *Journal of Proteome Research*, 18(8), 3142–3155. <https://doi.org/10.1021/acs.jproteome.9b00239>
 18. Kelley, D. E., Mookan, M., & Mandarino, L. J. (1992). Intracellular defects in glucose metabolism in obese patients with NIDDM. *Diabetes*, 41(6), 698–706. <https://doi.org/10.2337/diab.41.6.698>
 19. Song, R., Peng, W., Zhang, Y., Lv, F., Wu, H.-K., Guo, J., Cao, Y., Pi, Y., Zhang, X., Jin, L., Zhang, M., Jiang, P., Liu, F., Meng, S., Zhang, X., Jiang, P., Cao, C.-M., & Xiao, R.-P. (2013). Central role of E3 ubiquitin ligase MG53 in insulin resistance and metabolic disorders. *Nature*, 494(7437), 375–379. <https://doi.org/10.1038/nature11834>
 20. Hu, X., & Xiao, R.-P. (2018). MG53 and disordered metabolism in striated muscle. *Biochimica et Biophysica Acta (BBA) - Molecular Basis of Disease*, 1864(5 Pt B), 1984–1990. <https://doi.org/10.1016/j.bbadis.2017.10.013>
 21. Shiraishi, S., Zhou, C., Aoki, T., Sato, N., Chiba, T., Tanaka, K., Yoshida, S., Nabeshima, Y., Nabeshima, Y.-I., & Tamura, T.-A. (2007). TBP-interacting Protein 120B (TIP120B)/Cullin-associated and Neddylated-dissociated 2 (CAND2) inhibits SCF-dependent ubiquitination of myogenin and accelerates myogenic differentiation. *Journal of Biological Chemistry*, 282(12), 9017–9028. <https://doi.org/10.1074/jbc.M611513200>
 22. Wada, H., Kito, K., Caskey, L. S., Yeh, E. T. H., & Kamitani, T. (1998). Cleavage of the C-terminus of NEDD8 by UCH-L3. *Biochemical and Biophysical Research Communications*, 251(3), 688–692. <https://doi.org/10.1006/bbrc.1998.9532>
 23. Yang, S., Wang, B., Humphries, F., Hogan, A. E., O'shea, D., & Moynagh, P. N. (2014). The E3 ubiquitin ligase pellino3 protects against obesity-induced inflammation and insulin resistance. *Immunity*, 41(6), 973–987. <https://doi.org/10.1016/j.immuni.2014.11.013>
 24. Andersen, P. L., Zhou, H., Pastushok, L., Moraes, T., McKenna, S., Ziola, B., Ellison, M. J., Dixit, V. M., & Xiao, W. (2005). Distinct regulation of Ubc13 functions by the two ubiquitin-conjugating enzyme variants Mms2 and Uev1A. *Journal of Cell Biology*, 170(5), 745–755. <https://doi.org/10.1083/jcb.200502113>
 25. Xu, N., Gulick, J., Osinska, H., Yu, Y., McLendon, P. M., Shay-Winkler, K., Robbins, J., & Yutzy, K. E. (2020). Ube2v1 positively regulates protein aggregation by modulating ubiquitin proteasome system performance partially through K63 ubiquitination. *Circulation Research*, 126(7), 907–922. <https://doi.org/10.1161/circresaha.119.316444>
 26. Zhao, Y., Long, M. J. C., Wang, Y., Zhang, S., & Aye, Y. (2018). Ube2V2 is a rosetta stone bridging redox and ubiquitin codes, coordinating DNA damage responses. *ACS Central Science*, 4(2), 246–259. <https://doi.org/10.1021/acscentsci.7b00556>
 27. Pluska, L., Jarosch, E., Zaubner, H., Kniss, A., Waltho, A., Bagola, K., Von Delbrück, M., Löhr, F., Schulman, B. A., Selbach, M., Dötsch, V., & Sommer, T. (2021). The UBA domain of conjugating enzyme Ubc1/Ube2K facilitates assembly of K48/K63-branched ubiquitin chains. *The EMBO Journal*, 40(6), e106094. <https://doi.org/10.15252/embj.2020106094>
 28. Ohtake, F., Tsuchiya, H., Saeki, Y., & Tanaka, K. (2018). K63 ubiquitylation triggers proteasomal degradation by seeding branched ubiquitin chains. *Proceedings of the National Academy of Sciences*, 115(7), E1401–E1408. <https://doi.org/10.1073/pnas.1716673115>
 29. Hwang, H., Bowen, B. P., Lefort, N., Flynn, C. R., De Filippis, E. A., Roberts, C., Smoke, C. C., Meyer, C., Højlund, K., Yi, Z., & Mandarino, L. J. (2010). Proteomics analysis of human skeletal muscle reveals novel abnormalities in obesity and type 2 diabetes. *Diabetes*, 59(1), 33–42.
 30. Burniston, J. G. (2009). Adaptation of the rat cardiac proteome in response to intensity-controlled endurance exercise. *Proteomics*, 9(1), 106–115. <https://doi.org/10.1002/pmic.200800268>
 31. Li, J., Powell, S. R., & Wang, X. (2011). Enhancement of proteasome function by PA28 α overexpression protects against oxidative stress. *FASEB Journal*, 25(3), 883–893. <https://doi.org/10.1096/fj.10-160895>
 32. Merforth, S., Kuehn, L., Osmers, A., & Dahmann, B. (2003). Alteration of 20S proteasome-subtypes and proteasome activator PA28 in skeletal muscle of rat after induction of diabetes mellitus. *International Journal of Biochemistry, & Cell Biology*, 35(5), 740–748. [https://doi.org/10.1016/s1357-2725\(02\)00381-3](https://doi.org/10.1016/s1357-2725(02)00381-3)
 33. Haslbeck, M., Weinkauff, S., & Buchner, J. (2019). Small heat shock proteins: Simplicity meets complexity. *Journal of Biological Chemistry*, 294(6), 2121–2132. <https://doi.org/10.1074/jbc.REV118.002809>
 34. Gonçalves, C. C., Sharon, I., Schmeing, T. M., Ramos, C. H. I., & Young, J. C. (2021). The chaperone HSPB1 prepares protein aggregates for

- resolubilization by HSP70. *Scientific Reports*, 11(1), 17139. <https://doi.org/10.1038/s41598-021-96518-x>
35. Gupta, S., Deepti, A., Deegan, S., Lisbona, F., Hetz, C., & Samali, A. (2010). HSP72 protects cells from ER Stress-induced apoptosis via enhancement of IRE1 α -XBP1 Signaling through a Physical Interaction. *PLOS Biology*, 8(7), e1000410. <https://doi.org/10.1371/journal.pbio.1000410>
 36. Chung, J., Nguyen, A.-K., Henstridge, D. C., Holmes, A. G., Chan, M. H. S., Mesa, J. L., Lancaster, G. I., Southgate, R. J., Bruce, C. R., Duffy, S. J., Horvath, I., Mestrlil, R., Watt, M. J., Hooper, P. L., Kingwell, B. A., Vigh, L., Hevener, A., & Febbraio, M. A. (2008). HSP72 protects against obesity-induced insulin resistance. *Proceedings of the National Academy of Sciences*, 105(5), 1739–1744. <https://doi.org/10.1073/pnas.0705799105>
 37. Fernández-Fernández, M. R., & Valpuesta, J. M. (2018). Hsp70 chaperone: A master player in protein homeostasis. *F1000Res*, 7, F1000 Faculty Rev–1497. <https://doi.org/10.12688/f1000research.15528.1>
 38. Lee, J.-H., Gao, J., Kosinski, P. A., Elliman, S. J., Hughes, T. E., Gromada, J., & Kemp, D. M. (2013). Heat shock protein 90 (HSP90) inhibitors activate the heat shock factor 1 (HSF1) stress response pathway and improve glucose regulation in diabetic mice. *Biochemical and Biophysical Research Communications*, 430(3), 1109–1113. <https://doi.org/10.1016/j.bbrc.2012.12.029>
 39. Jing, E., Sundararajan, P., Majumdar, I. D., Hazarika, S., Fowler, S., Szeto, A., Gesta, S., Mendez, A. J., Vishnudas, V. K., Sarangarajan, R., & Narain, N. R. (2018). Hsp90 β knockdown in DIO mice reverses insulin resistance and improves glucose tolerance. *Nutrition, & Metabolism*, 15, 11. <https://doi.org/10.1186/s12986-018-0242-6>
 40. Venojärvi, M., Korkmaz, A., Aunola, S., Hällsten, K., Virtanen, K., Marniemi, J., Halonen, J.-P., Hänninen, O., Nuutila, P., & Atalay, M. (2014). Decreased thioredoxin-1 and increased HSP90 expression in skeletal muscle in subjects with type 2 diabetes or impaired glucose tolerance. *BioMed Research International*, 2014, 1–6. <https://doi.org/10.1155/2014/386351>
 41. Backe, S. J., Sager, R. A., Woodford, M. R., Makedon, A. M., & Mollapour, M. (2020). Post-translational modifications of Hsp90 and translating the chaperone code. *Journal of Biological Chemistry*, 295(32), 11099–11117. <https://doi.org/10.1074/jbc.REV120.011833>
 42. Beck, R., Dejeans, N., Glorieux, C., Creton, M., Delaive, E., Dieu, M., Raes, M., Levêque, P., Gallez, B., Depuydt, M., Collet, J.-F., Calderon, P. B., & Verrax, J. (2012). Hsp90 is cleaved by reactive oxygen species at a highly conserved N-terminal amino acid motif. *PLoS ONE*, 7(7), e40795. <https://doi.org/10.1371/journal.pone.0040795>
 43. Gesualdi, N. M., Chirico, G., Pirozzi, G., Costantino, E., Landriscina, M., & Esposito, F. (2007). Tumor necrosis factor-associated protein 1 (TRAP-1) protects cells from oxidative stress and apoptosis. *Stress (Amsterdam, Netherlands)*, 10(4), 342–350. <https://doi.org/10.1080/10253890701314863>
 44. Richarme, G., Mihoub, M., Dairou, J., Bui, L. C., Leger, T., & Lamouri, A. (2015). Parkinsonism-associated protein DJ-1/park7 is a major protein deglycase that repairs methylglyoxal- and glyoxal-glycated cysteine, arginine, and lysine residues. *Journal of Biological Chemistry*, 290(3), 1885–1897. <https://doi.org/10.1074/jbc.M114.597815>
 45. Mey, J. T., Blackburn, B. K., Miranda, E. R., Chaves, A. B., Briller, J., Bonini, M. G., & Haus, J. M. (2018). Dicarbonyl stress and glyoxalase enzyme system regulation in human skeletal muscle. *American Journal of Physiology, Regulatory, Integrative and Comparative Physiology*, 314(2), R181–R190. <https://doi.org/10.1152/ajpregu.00159.2017>
 46. Xia, Q., Casas-Martinez, J. C., Zarzuela, E., Muñoz, J., Miranda-Vizuete, A., Goljanek-Whysall, K., & McDonagh, B. (2023). Peroxiredoxin 2 is required for the redox mediated adaptation to exercise. *Redox Biology*, 60, 102631. <https://doi.org/10.1016/j.redox.2023.102631>
 47. Brinkmann, C., Chung, N., Schmidt, U., Kreutz, T., Lenzen, E., Schiffer, T., Geisler, S., Graf, C., Montiel-Garcia, G., Renner, R., Bloch, W., & Brixius, K. (2012). Training alters the skeletal muscle antioxidative capacity in non-insulin-dependent type 2 diabetic men. *Scandinavian Journal of Medicine, & Science in Sports*, 22(4), 462–470. <https://doi.org/10.1111/j.1600-0838.2010.01273.x>
 48. Al-Khalili, L., De Castro Barbosa, T., Östling, J., Massart, J., Katayama, M., Nyström, A.-C., Oscarsson, J., & Zierath, J. R. (2013). Profiling of human myotubes reveals an intrinsic proteomic signature associated with type 2 diabetes. *Biochemical Pharmacology*, 2, 25–38. <https://doi.org/10.1016/j.trprot.2013.12.002>
 49. Tran, L., Langlais, P. R., Hoffman, N., Roust, L., & Katsanos, C. S. (2019). Mitochondrial ATP synthase β -subunit production rate and ATP synthase specific activity are reduced in skeletal muscle of humans with obesity. *Experimental Physiology*, 104(1), 126–135. <https://doi.org/10.1113/ep087278>
 50. Perez-Riverol, Y., Csordas, A., Bai, J., Bernal-Llinares, M., Hewapathirana, S., Kundu, D. J., Inuganti, A., Griss, J., Mayer, G., Eisenacher, M., Pérez, E., Uszkoreit, J., Pfeuffer, J., Sachsenberg, T., Yilmaz, S., Tiwary, S., Cox, J., Audain, E., Walzer, M., ... Vizcaino, J. A. (2019). The PRIDE database and related tools and resources in 2019: Improving support for quantification data. *Nucleic Acids Research*, 47(D1), D442–D450. <https://doi.org/10.1093/nar/gky1106>

SUPPORTING INFORMATION

Additional supporting information may be found online <https://doi.org/10.1002/pmic.202300395> in the Supporting Information section at the end of the article.

How to cite this article: Srisawat, K., Stead, C. A., Hesketh, K., Pogson, M., Strauss, J. A., Cocks, M., Siekmann, I., Phillips, S. M., Lisboa, P. J., Shepherd, S., & Burniston, J. G. (2023). People with obesity exhibit losses in muscle proteostasis that are partly improved by exercise training. *Proteomics*, e2300395. <https://doi.org/10.1002/pmic.202300395>